Hindawi
Complexity
Volume 2020, Article ID 2498073, 14 pages
https://doi.org/10.1155/2020/2498073

Research Article

Regular and Irregular Vegetation Pattern Formation in Semiarid Regions: A Study on Discrete Klausmeier Model

Huayong Zhang,[1] **Tousheng Huang**,[1] **Liming Dai**,[2] **Ge Pan**,[1] **Zhao Liu**,[1] **Zichun Gao**,[1] **and Xiumin Zhang**[1]

[1]*Research Center for Engineering Ecology and Nonlinear Science, North China Electric Power University, Beijing 102206, China*
[2]*Industrial Systems Engineering, University of Regina, Regina, SK S4S 0A2, Canada*

Correspondence should be addressed to Huayong Zhang; rceens@ncepu.edu.cn

Received 17 March 2019; Accepted 21 July 2019; Published 8 January 2020

Academic Editor: Dan Selişteanu

The research on regular and irregular vegetation pattern formation in semiarid regions is an important field in ecology. Applying the framework of coupled map lattice, a novel nonlinear space- and time-discrete model is developed based on discretizing the classical Klausmeier model and the vegetation pattern formation in semiarid regions is restudied in this research. Through analysis of Turing-type instability for the discrete model, the conditions for vegetation pattern formation are determined. The discrete model is verified by Klausmeier's results with the same parametric data, and shows advantages in quantitatively describing diverse vegetation patterns in semiarid regions, such as the patterns of regular mosaicirregular patches, stripes, fractured stripesspots, and stripes-spots, in comparing with former theoretical models. Moreover, the discrete model predicts variations of rainfall and vegetation types can cause transitions of vegetation patterns. This research demonstrates that the nonlinear mechanism of the discrete model better captures the diversity and complexity of vegetation pattern formation in semiarid regions.

1. Introduction

The regular and irregular spatial vegetation patterns are very important landscapes widely distributed in semiarid regions [1–4]. Due to insufficiency of water resource, the vegetation cover may hardly maintain homogeneous and may be self-organized into heterogeneous vegetation patches [5]. In recent decades, the vegetation pattern formation in semiarid regions has aroused widespread interests of theoretical and experimental ecologists [6–11].

Many studies suggest that the formation of vegetation patterns in semiarid regions results from feedbacks between biomass and water resource [5, 12–14]. Based on the feedbacks, a great number of mathematical models have been established [9]. Among these models, the Klausmeier model [13] plays an important role. Many models developed later can be considered as modified versions of the Klausmeier model [15–18].

The Klausmeier model is a continuous dynamic model with vegetation biomass and water resource as state variables. This model provides a classical combination of ecological and nonlinear mechanisms in determining the vegetation pattern formation in semiarid regions. It grasps the feature of interactions between plant and water, capturing the formation of striped vegetation patterns on hillslopes. Klausmeier's work has a close agreement with field observations. With the employment of the Klausmeier model, the wavelength and migration speed of the striped patterns on hillslopes are predicted [19]. Systematic investigations on the pattern solutions of the Klausmeier model provide more predictions for the nonlinear characteristics of striped vegetation in semiarid environments [20–22].

As so far, most of the spatially extended models in literature researching the vegetation pattern formations are time- and space-continuous [9, 23]. However, the continuous dynamic models simplify the fact that natural ecological systems composing of separate individuals are often patchy and exhibit discontinuous properties [24, 25]. Correspondingly, it should be more reasonable and adequate applying discrete models to study the discontinuous vegetation in ecological systems [25]. It is widely recognized that discrete dynamic models show effectiveness and power in

describing nonlinear characteristics and complexity of natural ecological systems. Domokos and Scheuring [26] found that the discrete model can be more accurate than corresponding continuous model in describing population dynamics. Han et al. [27] and Li et al. [28] discovered that Turing instability and Turing patterns can occur in the discrete rather than the corresponding continuous competitive Lotka–Volterra system. The discrete Logistic system can generate chaos which has great significance in describing the complexity of population dynamics [29, 30]. A lot of research works have demonstrated that the application of discrete dynamic models may lead to better results in studying ecological systems [31, 32].

In literature, the discrete models for studying vegetation patterns have a few types, including cellular automata, metapopulation models, coupled map lattices, and so on [9, 12, 33, 34]. In this research, the space- and time-discrete model of vegetation pattern formation will be given by a coupled map lattice. The coupled map lattices are characterized by discrete time, discrete space, and continuous states, and are comparable with two other standard models for spatially extended dynamical systems, namely, partial differential equations and cellular automata [34]. They have great advantages in describing the spatiotemporal chaos and are widely applied in many fields [35]. In ecology, the application of coupled map lattices results in a better understanding and prediction of ecological complexities of pattern formations [25, 34, 35]. However, scarce coupled map lattice model is documented in literature for quantitatively describing the vegetation pattern formation in semiarid regions, and a reliable one is still needed. Referring to the research works on difference equation models [36, 37], the new model can be developed from discretizing a continuous model. Due to the importance of Klausmeier model in vegetation pattern formation studies, it is ecologically representative to apply the discretization of the Klausmeier model.

This research focuses on the self-organized patterns resulting from Turing-type instability mechanism, i.e., Turing-type patterns [9, 13]. The Turing instability was initially found by Turing [38] and the theory of Turing instability has been widely employed and further improved in ecology to investigate the pattern formation [5] and [19]. New types of Turing instability (collectively called Turing-type instability) are found, such as differential flow instability [13], cross-diffusion driven instability [39], and so on. Generally, the mechanism for occurrence of Turing-type instability is spatial symmetry breaking at the spatially homogeneous state [9].

In this research, a nonlinear space- and time-discrete model of water and biomass is to be developed for quantitatively describing the vegetation pattern formation in semiarid regions, on the basis of discretizing the Klausmeier model. Via analyzing the Turing-type instability for the discrete model, the occurrence conditions of vegetation patterns are to be analytically determined. Numerical simulations are to be performed under the occurrence conditions of Turing-type patterns, to demonstrate the formation of diverse and complex vegetation patterns in semiarid regions.

2. Development of space- and Time-Discrete Model

The Klausmeier model was established in 1999 for investigating the formation of vegetation patterns in semiarid regions. The model grasps the feature of interactive mechanism of biomass and water, and predicts vegetation patterns which have close agreement with observations [13, 19]. The model has two state variables, water and vegetation biomass. The dynamics of water is a process of water redistribution. On one hand, rainfall water is depleted by evaporation and plant absorption; on the other hand, the water flows downslope. The dynamics of biomass is described by vegetation growth, natural mortality, and lateral diffusion (see Figure 1(a)). The governing equations of the Klausmeier model are expressed by:

$$\frac{\partial W}{\partial T} = A - LW - RWU^2 + V\frac{\partial W}{\partial X}, \tag{1a}$$

$$\frac{\partial U}{\partial T} = RJWU^2 - MU + D\left(\frac{\partial^2 U}{\partial X^2} + \frac{\partial^2 U}{\partial Y^2}\right), \tag{1b}$$

in which W (kg H_2O m^{-2}) is water amount and U (kg dry mass m^{-2}) is vegetation biomass; T (year) is time and X (m) and Y (m) index a two-dimensional domain; negative X direction is the downslope water flow direction on hillslopes, and Y direction is the latitudinal direction; A (kg H_2O m^{-2} $year^{-1}$) is rainfall rate, L($year^{-1}$) is evaporation rate of water; R ((kg m^{-2})$^{-2}$ $year^{-1}$) describes the rate of per unit vegetation biomass taking up water, J ((kg dry mass) (kg H_2O)$^{-1}$) expresses the conversion rate of vegetation biomass from per unit water consumed; M ($year^{-1}$) is mortality rate of vegetation biomass; V (m $year^{-1}$) is the flow speed of water downslope, and D (m^2 $year^{-1}$) is the diffusion coefficient of vegetation dispersal, describing the diffusion capability of the vegetation.

The Klausmeier model can be nondimensionalized and transformed into a dimensionless form,

$$\frac{\partial w}{\partial t} = a - w - wu^2 + v_0\frac{\partial w}{\partial x}, \tag{2a}$$

$$\frac{\partial u}{\partial t} = wu^2 - mu + \left(\frac{\partial^2}{\partial x^2} + \frac{\partial^2}{\partial y^2}\right)u, \tag{2b}$$

using following nondimensionalized expressions,

$$\begin{aligned} w &= R^{1/2}L^{-1/2}JW, \\ u &= R^{1/2}L^{-1/2}U, \\ t &= LT, \\ x &= L^{1/2}D^{-1/2}X, \\ y &= L^{1/2}D^{-1/2}Y, \\ a &= AR^{1/2}L^{-3/2}J, \\ m &= ML^{-1}, \\ v_0 &= VL^{-1/2}D^{-1/2}, \end{aligned} \tag{3}$$

in which a controls the water input through precipitation, m measures the biomass mortality, and v_0 controls the rate at which water flows downslope.

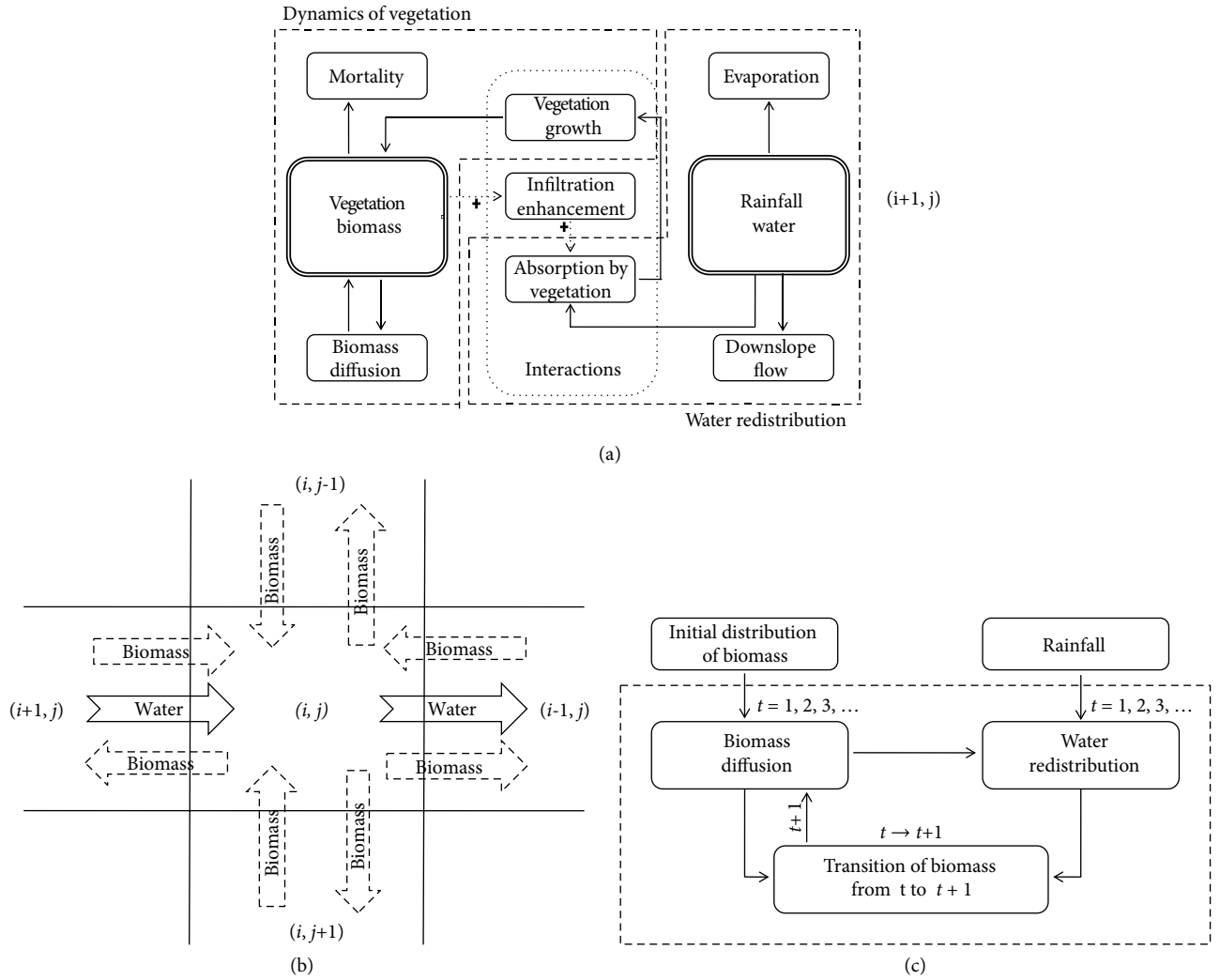

FIGURE 1: Outlines for (a) the Klausmeier's model, (b) biomass diffusion and water flow in discrete space, and (c) the coupled map lattice model.

On the basis of the Klausmeier model described by Eq. (2), a space- and time-discrete model of water and biomass, which is given by a coupled map lattice, is developed. Like many research works in literature, a common method for develing discrete model, discretizing the continuous model, is applied [36, 37]. We divide the spatial domain into $n \times n$ cells and the time into a sequence of time intervals. Using w_t^{ij} and u_t^{ij} to represent water amount and vegetation biomass in the cell (i, j) at tth time interval. According to literature, the dynamics of a coupled map lattice consists of two alternating stages, the temporal nonlinear "reaction" stage and the spatial movement stage [25, 34, 35, 40–42]. Corresponding to the ecological framework of Klausmeier's work (see Figure 1(a)), the spatial movement includes biomass diffusion, water flow (see Figure 1(b)), and water redistribution resulting from water flow on hillslopes. The "reaction" stage is represented by plant growth, which occurs in turn after the biomass diffusion and the water redistribution. One can see the outline in Figure 1(c) for the details of the coupled map lattice model in this research. In the outline, we determine the biomass diffusion and water redistribution firstly and then the transition of vegetation biomass from time t to time $t + 1$. It should be noticed that such sequential determination agrees with the natural processes in ecological systems and is not described by the Klausmeier model [34].

With consideration of biomass diffusion, u_t^{ij} will change to a new vegetation biomass, $\overline{u}_t^{ij}$. Applying discretization on the diffusion term of Eq. (2b), $\overline{u}_t^{ij}$ can be obtained as

$$\overline{u}_t^{ij} = u_t^{ij} + d\nabla_D^2 u_t^{ij}, \tag{4a}$$

In which

$$d = \frac{t_h}{s_h^2}, \tag{4b}$$

$$\nabla_D^2 u_t^{ij} = u_t^{i+1,j} + u_t^{i,j+1} + u_t^{i-1,j} + u_t^{i,j-1} - 4u_t^{ij}, \tag{4c}$$

where t_h measures the duration of one time interval, s_h measures the length of one cell, ∇_D^2 denotes the discrete version of Laplacian operator ∇^2 and describes the diffusion in discrete space (see Figure 1(b)).

The water redistribution is then considered. Discretizing Eq. (2a), we have the following equation,

$$w_{t+1}^{ij} = w_t^{ij} + t_h\left(a - w_t^{ij} - w_t^{ij}\left(u_t^{ij}\right)^2\right) + \nu\nabla w_t^{ij}, \quad (5a)$$

in which

$$\nu = \frac{t_h \nu_0}{s_h}, \quad (5b)$$

$$\nabla_D w_t^{ij} = w_t^{i+1,j} - w_t^{ij}. \quad (5c)$$

Likewise, ∇_D is the discrete version of operator ∇ and describes the flow in discrete space (see Figure 1(b)). In this research, we set $t_h = 1$, and hence the water input in the ecological system maintains as a in every time interval. Two aspects should be taken into consideration correspondingly. First, the precipitation water is completely depleted in one time interval; second, the vegetation biomass involving in the water redistribution is $\overline{u}_t^{ij}$ due to the biomass diffusion. On this basis, Eq. (5a) is modified and the discrete equation of the water redistribution can be obtained as,

$$0 = a - w_t^{ij} - w_t^{ij}\left(\overline{u}_t^{ij}\right)^2 + \nu\nabla w_t^{ij}. \quad (6)$$

In its turn, applying the space- and time-discretization on Eq. (2b), the "reaction" stage of plant growth can be described by

$$u_{t+1}^{ij} = \overline{u}_t^{ij} + t_h\left(w_t^{ij}\left(\overline{u}_t^{ij}\right)^2 - m\overline{u}_t^{ij}\right). \quad (7)$$

Rewrite the above equations, the space- and time-discrete model for vegetation pattern formation in semiarid regions can be described by the following,

$$0 = a - w_t^{ij} - w_t^{ij}\left(u_t^{ij} + d\nabla_D^2 u_t^{ij}\right)^2 + \nu\nabla_D w_t^{ij}, \quad (8a)$$

$$u_{t+1}^{ij} = (1-m)\left(u_t^{ij} + d\nabla_D^2 u_t^{ij}\right) + w_t^{ij}\left(u_t^{ij} + d\nabla_D^2 u_t^{ij}\right)^2. \quad (8b)$$

The spatial dynamics of water and vegetation in the boundary cells are provided by boundary conditions. Like in Klausmeier [13], periodic boundary conditions are applied in this research and described as the following,

$$\begin{aligned} w_t^{i,0} &= w_t^{i,n}, \\ w_t^{i,1} &= w_t^{i,n+1}, \\ w_t^{0,j} &= w_t^{n,j}, \\ w_t^{1,j} &= w_t^{n+1,j}, \end{aligned} \quad (8c)$$

$$\begin{aligned} u_t^{i,0} &= u_t^{i,n}, \\ u_t^{i,1} &= u_t^{i,n+1}, \\ u_t^{0,j} &= u_t^{n,j}, \\ u_t^{1,j} &= u_t^{n+1,j}. \end{aligned} \quad (8d)$$

In all the equations above, $i, j \in \{1, 2, 3, \ldots, n\}$, $t \in Z^+$, and n in the equations is a positive integer.

The discrete model restates the interactions of water and vegetation from the view of discrete time and space. In the following, the discrete model is investigated to quantitatively determine the vegetation pattern formation in semiarid regions.

3. Conditions for Turing-Type Pattern Formation

The occurrence of Turing-type patterns requires two conditions [5, 9, 38]. First, a nontrivial spatially homogeneous stationary state exists and is stable to spatially homogeneous perturbations. Second, this stable stationary state is unstable to at least one type of spatially heterogeneous perturbations. The second condition defines the condition for Turing-type instability, which ensures local perturbations on the stable homogeneous stationary state gradually expand globally.

3.1. Conditions for Stable Homogeneous Stationary State. According to the conditions for Turing-type patterns, the spatially homogeneous stationary states of the discrete model are studied at first. The homogeneous stationary states demand $\nabla_D w_t^{ij} \equiv 0$ and $\nabla_D^2 u_t^{ij} \equiv 0$, for all of i and j. With the calculation as described in Appendix A, three spatially homogeneous stationary states can be obtained when $a > 2m$,

$$(w_0, u_0) : (a, 0); \quad (9a)$$

$$(w_1, u_1) : \left(\frac{a + \sqrt{a^2 - 4m^2}}{2}, \frac{2m}{a + \sqrt{a^2 - 4m^2}}\right), \quad (9b)$$

$$(w_2, u_2) : \left(\frac{a - \sqrt{a^2 - 4m^2}}{2}, \frac{2m}{a - \sqrt{a^2 - 4m^2}}\right), \quad (9c)$$

(w_0, u_0) represents the state of bare ground without vegetation pattern formation and will not be further considered. The other two states (w_1, u_1) and (w_2, u_2), describe homogeneous vegetation and will be discussed in below for the vegetation pattern formation.

The local stability of the homogeneous stationary states reflects how the system resists spatially homogeneous perturbations. If the state is locally stable, the system may return to this state after the occurrence of homogeneous perturbations. Such property ensures the convergence of the system and is important for the vegetation pattern formation. Based on the calculation in Appendix A, the conditions for stable homogeneous state (w_2, u_2) are determined as the following,

$$\text{Case (1)} : m \le 2,\ a > 2m; \quad (10a)$$

$$\text{Case (2)} : m > 2,\ 2m \le a < \frac{2m^2}{\sqrt{m^2 - 4}}. \quad (10b)$$

Figure 2 shows the stable homogeneous state occurring in the temporal evolution of vegetation density, when the parameters satisfy the conditions described in Eq. (10a). As shown in Figure 2, the trajectory asymptotically approaches (w_2, u_2).

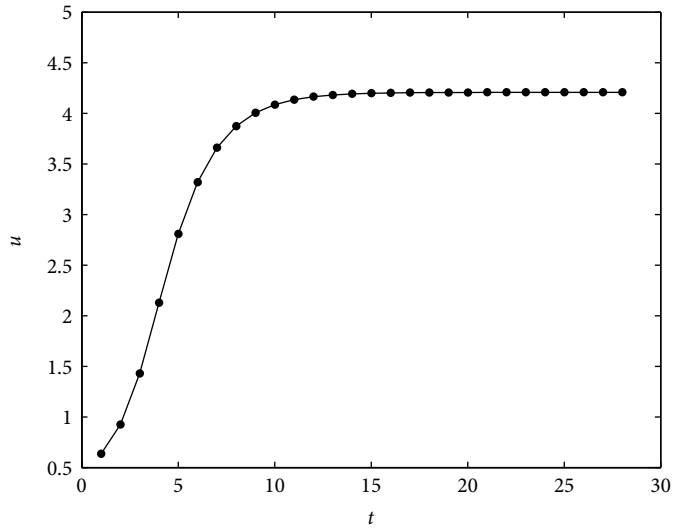

Figure 2: Stable stationary state of the discrete model when conditions in Eq. (10a) are satisfied $a = 2$, $m = 0.45$.

However, it should be noticed that (w_2, u_2) is locally asymptotically stable rather than globally stable. If the initial value of u is too low (for example, lower than u_1), the discrete system will evolve into bare ground.

3.2. Condition for Turing-Type Instability. According to the results obtained above, the analysis of Turing-type instability is further performed on the stable homogeneous stationary state represented by (w_2, u_2). Spatially heterogeneous perturbations are introduced to the discrete model and observe the behaviors of the model system. When vegetation biomass and/or water resource are enhanced or reduced spatially heterogeneously by the perturbations, the discrete system may converge to two states as the time progresses. The first is the homogeneous state, this case suggests that the system can resist the heterogeneous perturbations as well and homogenous vegetation dominates. If the homogeneous state becomes unstable under the heterogeneous perturbations, the system will converge to another state with spatially heterogeneous vegetation, demonstrating the vegetation pattern formation. With the calculations in Appendix B, we can summarize the effect of heterogeneous perturbations around the global space. This leads to the following dynamic equations:

$$0 = \left(a_{11} - v\lambda_{kl}^{(1)}\right)W_t + a_{12}\left(1 - d\lambda_{kl}^{(2)}\right)U_t, \tag{11a}$$

$$U_{t+1} = a_{21}W_t + a_{22}\left(1 - d\lambda_{kl}^{(2)}\right)U_t. \tag{11b}$$

Eq. (11) describes the dynamics of spatially heterogeneous perturbations in entire space. If Eq. (11) converges, the system will go back to the spatially homogeneous stationary state. Only the divergence of Eq. (11) can lead to the breaking of the homogeneous state and the formation of Turing-type patterns. Eq. (11) can be transformed into the following form,

$$U_{t+1} = \left(\frac{a_{12}a_{21}}{v\lambda_{kl}^{(1)} - a_{11}} + a_{22}\right)\left(1 - d\lambda_{kl}^{(2)}\right)U_t. \tag{12}$$

That Eq. (12) diverges needs the satisfaction of following condition, i.e., existing at least one group of k and l to make

$$Z(k,l) = \left|\left(\frac{a_{12}a_{21}}{v\lambda_{kl}^{(1)} - a_{11}} + a_{22}\right)\left(1 - d\lambda_{kl}^{(2)}\right)\right| > 1. \tag{13}$$

Eq. (13) gives the condition for Turing-type instability of the discrete model. Such condition is obtained when weak spatially heterogeneous perturbations take place around the stable homogeneous state.

Given the above calculations, the occurrence of Turing-type patterns for the discrete model demands the parameter values satisfy the conditions described in either Eq. (10a) or Eq. (10b), combined with the condition in Eq. (13). The Conditions of Turing-type patterns determine the parameter space for vegetation pattern formation. Under the conditions obtained, the vegetation pattern formation in semiarid regions can be quantitatively studied by numerical simulations.

4. Numerical Simulations and Discussion

Numerical simulations are performed to mimic the formation of vegetation patterns in semiarid regions. Since the vegetation pattern formation for the discrete model is still based on Klausmeier's ecological framework, the same parameter values/range in Klausmeier [13] are applied. With application of the parametric data in Table 1, validation of vegetation pattern formation is performed firstly to prove the feasibility of the discrete model.

Using the nondimensionalized expressions described previously, the values/range for the scaling parameters in the discrete model can be obtained (see Table 2). Simultaneously, the values of other parameters used in the discrete model are also given in Table 2. To compare with the results shown in Klausmeier [13], Figure 3 is plotted with $a = 2$, $m = 0.45$, and length of cell at 2 m (noticing that the cell length equals $s_h L^{-1/2} D^{1/2}$ according to Eq. (3)).

Table 1: Parameter values/range used in Klausmeier [13].

Parameter	A	L	R		J		M		V	D
			R_{grass}	R_{tree}	J_{grass}	J_{tree}	M_{grass}	M_{tree}		
Unit	kg H_2O m^{-2} $year^{-1}$	$year^{-1}$	$(kg\ m^{-2})^{-2}\ year^{-1}$		(kg dry mass) $(kg\ H_2O)^{-1}$		$year^{-1}$		m $year^{-1}$	$m^2\ year^{-1}$
Value/range	250~750	4	100	1.5	0.003	0.002	1.8	0.18	365	1

Table 2: Values/ranges and scaling for the parameters of the discrete model.

Parameter	a		m		t_h	S_h	d	v	n
	a_{grass}	a_{tree}	m_{grass}	m_{tree}					
Scaling	$AR^{1/2}L^{-3/2}J$		ML^{-1}		—	—	$t_h S_h^{-2}$	$VL^{-1/2}D^{-1/2}\,t_h S_h^{-1}$	—
Value/range	0.94~2.81	0.091~0.23	0.45	0.045	1	4	0.0625	45.625	50

Figure 3(a) shows the vegetation pattern evolving during the transient dynamics ($t = 100$). In Figure 3(a), vegetation strips emerge in the form of forks and dead-ends. After the transient dynamics ($t = 1000$), regular vegetation stripes take place, perpendicular to the downslope direction, as shown in Figure 3(b). Figure 3 shows the same formation process of vegetation pattern with that described in Klausmeier [13]. Moreover, the wavelength for the vegetation pattern shown in Figure 3(b) is about 14.29 m, which is close to the wavelength simulated by Klausmeier, 12.5 m. These agreements suggest that the discrete model can repeat the vegetation pattern formation of the Klausmeier model.

Figure 3(c) shows the influence of cell length and cell numbers on the pattern formation. The cell length and the cell numbers define the domain scale for vegetation pattern formation. When the cell length is given in range of 1~3 m, the wavelength fluctuates around 13.5~15.5 m. Both $n = 50$ and $n = 100$ can lead to the same result, which suggests the steadiness of pattern formation with the change of domain scale. The cell length is important for measuring the vegetation pattern formation. As described in literature, many dynamic models show suitable cell sizes for simulating vegetation pattern formation [43, 44]. Under the parametric conditions given in Table 2, the suitable cell length for the discrete model ranges in 1~3 m. Therefore, applying cell-length = 2 m and $n = 50$ (the domain scale is 100 m×100 m) is reasonable for simulating the vegetation pattern formation of the discrete model.

The vegetation pattern self-organized on hillslopes has two important properties, wavelength and upslope migrating. With the values/ranges for the parameters provided in Table 2, the ranges of wavelength and migrating speed for the vegetation patterns in semiarid regions (250~750 kg H_2O $m^{-2}\,year^{-1}$) are got (see Table 3). As shown in Table 3, the wavelength range for the vegetation stripes agrees with Klausmeier's results. Moreover, with the comparison shown in Table 3, our result of migrating speed of grass stripes (0.6~1.1) is closer to field observation (0.3~1.5) than Klausmeier's results (1.4~1.9).

The validation of the discrete model shows the formation of banded vegetation pattern on hillslopes, characteristics of which have agreement with Klausmeier's results and field observation. These results prove the feasibility of applying the discrete model in studying the vegetation pattern formation in semiarid regions. In the following, further numerical simulations are performed to demonstrate the vegetation pattern formation of the discrete model as parametric conditions shift. The parameter ranges/values given in Table 2 are still used, except that values of parameters a and d may change. Two initial vegetation conditions are applied corresponding to weak perturbations and strong perturbations described in Section 3.

(a) *Initial condition 1 (IC1):* weak perturbations at the stable homogeneous vegetation. The initial vegetation value for the ijth lattice is described by $u_0^{ij} = (1 + 0.1(\xi - 0.5))u_2$, in which ξ follows standard uniform distribution. This condition is only applied when Eq. (27) establishes.

(b) *Initial condition 2 (IC2):* strong perturbations. Randomly selecting 30% (other percentages are also suitable) cells, the initial vegetation value in each of these cells is set as ξu_2, whereas the other cells are defined as bare ground.

The above parametric and initial conditions are given under the Turing-type pattern formation conditions described in Section 3. Based on these conditions, following numerical simulations are performed. Corresponding to Klausmeier's work, two cases of vegetation pattern formation are studied, $v = 0$ (on flat ground) and $v \gg 0$ (on hillslopes).

4.1. $v = 0$: Vegetation Pattern Formation on Flat Ground. The numerical solutions of Eq. (8) with $v = 0$ describes the vegetation pattern formation on flat ground. Figure 4 shows the regular mosaic vegetation pattern self-organized when the value of D is given at 5.6 ($m^2\ year^{-1}$). In the pattern, the vegetation interweaves with the bare ground. Each vegetated patch is surrounded by four areas of bare ground. In appearance, the mosaic pattern is close to the natural gap patterns, which are described by [43, 45, 46].

In the research work of Klausmeier [13], the irregular mosaic vegetation pattern is also obtained. However in Klausmeier's work, the occurrence of vegetation patterns on

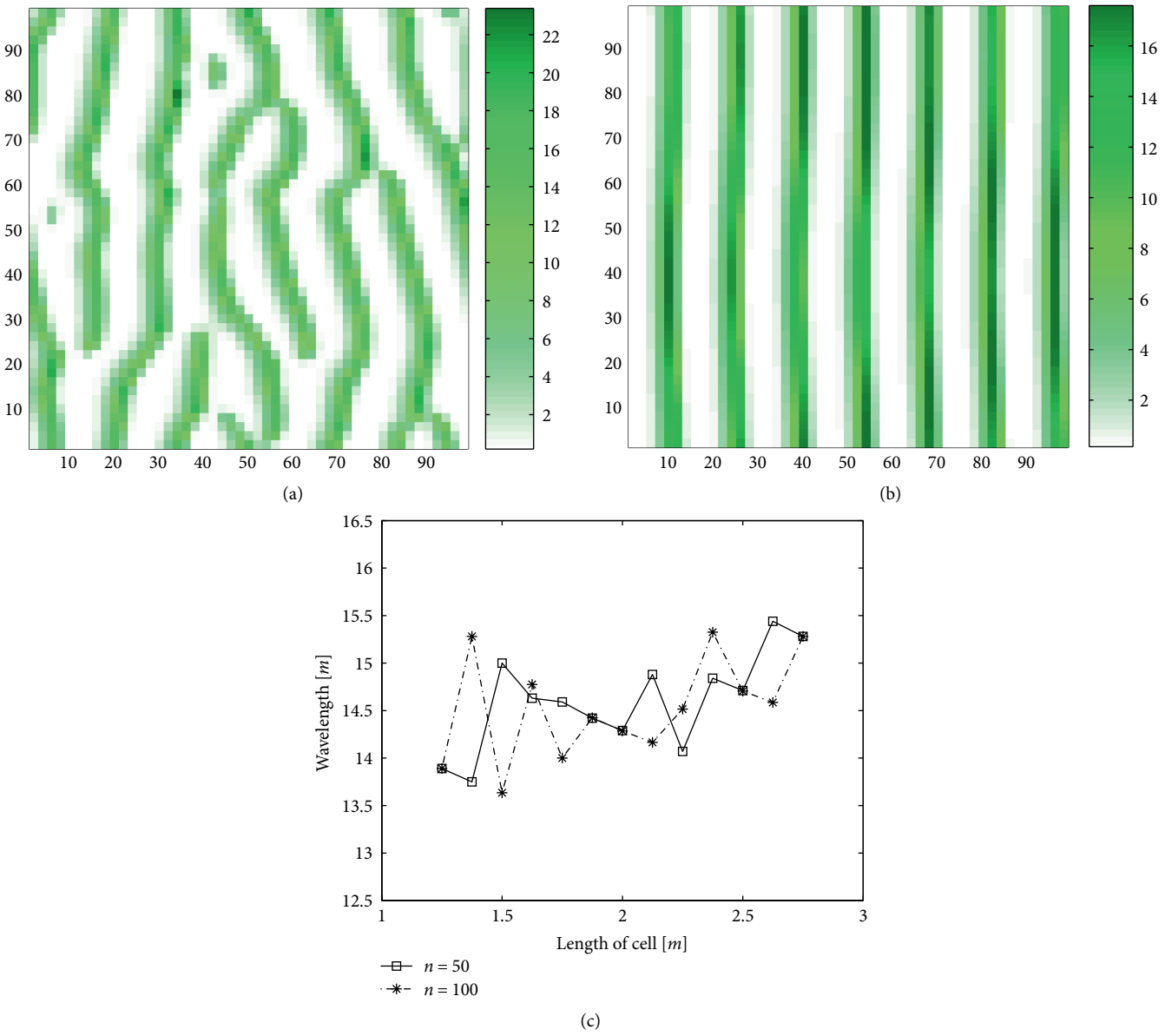

Figure 3: Validation for simulating vegetation pattern formation of the discrete model, with application of same parameter values in Klausmeier [13]. $a = 2$, $m = 0.45$, and the other parameter values is given in Table 2. (a) and (b) are the vegetation patterns at $t = 100$ and $t = 1000$, the downslope direction is set from left to right, (c) change of pattern wavelength with the cell length.

Table 3: Comparison of ranges of wavelength and migrating speed for striped vegetation patterns.

Property of vegetation stripes	Tree stripes		Grass stripes	
	Wavelength (m)	Migrating speed (m year^{-1})	Wavelength (m)	Migrating speed (m year^{-1})
Present result	25~68	0.6~1.9	10.5~28.6	0.6~1.1
Klausmeier's result	23~67	0.4~0.6	8.1~28	1.4~1.9
Field Observation*	70~190	0.15~0.3	1~40	0.3~1.5

*The data of field observation are obtained from Klausmeier [13].

flat ground is under unrealistic parameter values. Compared with Klausmeier's result, such disadvantage is removed in the vegetation pattern formation of the discrete model. The parameter values applied in Figure 4 and the corresponding self-organized pattern has realistic ecological significance, based on the comparison with the literature [13, 43, 45].

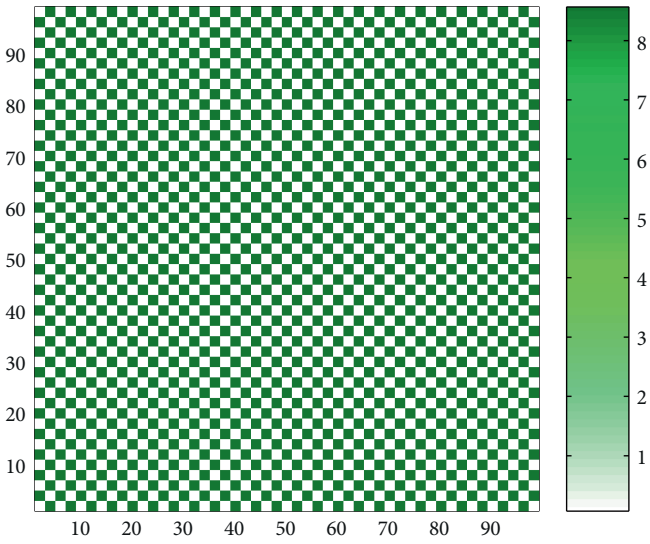

Figure 4: Regular mosaic vegetation pattern self-organized on flat ground, with application of IC1 or IC2 $a = 2$, $m = 0.45$, $d = 0.35$, $t = 800$.

Figure 5 is plotted to show the vegetation patterns of irregular patches on the flat ground. The formation of three patterns in Figure 5 is under the same initial condition (IC2). In these patterns, the vegetation patches appear in the forms of spots, stripes, and clusters. Each pattern composes of many vegetation patches and shows irregularity. The irregularity exhibits in two aspects, irregular distribution and irregular shapes of the vegetation patches. The patched vegetation patterns are widely discovered in field observation, such as the description by Cerdà [47]. However, such patterns cannot be predicted by the Klausmeier model.

The three patterns shown in Figure 5 demonstrate a transition of vegetation patterns along rainfall gradient ($A = 400$, 480, and 546 kg H_2O m^{-2} $year^{-1}$). As shown in Figure 5, the transition is from pattern of spots to pattern of clusters. Increase in the rainfall rate promotes the enlargement of vegetation patches in the patterns. As the rainfall rate continues growing (for example $a > 2.1$), spatially homogeneous vegetation dominates. As widely recognized, the competition for limited water resource in ecosystems plays an important role in the formation and transition of spatially heterogeneous vegetation patterns [8, 9]. Nevertheless, the increase of rainfall alleviates the pressure of competition between plant individuals and stimulates vegetation growth, giving rise to the transition of vegetation patterns.

Many models predict the transitions of vegetation patterns on flat ground along the rainfall gradient [15, 17, 43]. As described in literature, the vegetation experiences transitions from spotted pattern, to labyrinths and to gap pattern with the increase instriped vegetation patterns rainfall rate [43, 48, 49]. In this research, the discrete model predicts a different transition of vegetation patterns, as described in Figure 5. The difference may result from the effects of facilitative interactions between plant individuals, which limit soil moisture losses and result to the enlargement of vegetation patches [45, 50].

Klausmeier [13] introduced slight topographic variation to explain the vegetation pattern formation on flat ground. Compared with Klausmeier's work, the discrete model developed in this research makes an improvement. The pattern formation on flat ground and the pattern characteristics are essentially captured by the nonlinear mechanisms of the discrete model, without introduction of external excitations. This manifests the discrete model exhibits possibilities for reproducing new vegetation pattern formation and new pattern transition on the flat ground.

4.2. $v \gg 0$: Vegetation Pattern Formation on Hillslopes. For the discrete model, $v \gg 0$ means hillslope terrains and the value of v determines the hillslope gradient. In this subsection, the vegetation patterns self-organized on hillslopes are investigated. For comparing with Klausmeier's results, the same hillslope gradient in Klausmeier [13] is also applied ($V = 365$ m $year^{-1}$).

As shown in Figure 6, the discrete model can demonstrate the formation of many irregular vegetation patterns on hillslopes. With variation of parametric conditions, we find irregular vegetation patterns of curved stripes, fractured stripes, spots and stripes-spots. Most of dynamic models (including the Klausmeier model) are incapable of describing these patterns on hillslopes simultaneously. This reflects the advantage of the discrete model in quantitatively describing abundant patterns.

Figures 6(a)–(d) show the irregularly striped vegetation patterns, which appear as curved or fractured stripes. The striped vegetation patterns are a characteristic feature of landscapes in many semiarid regions [4]. A great number of dynamic models have been raised to predict the striped vegetation pattern formation [13, 43, 44]. Many continuous models such as the Klausmeier model predict that the vegetation stripes will finally stabilize at a state in which the vegetation stripes are strictly perpendicular to the waterflow direction, whereas the irregular stripes are explained as transient dynamics [44]. In such situation, environmental noises are often used to explain the maintenance of stable irregular patterns. However, the formation of irregular patterns is essentially from the nonlinear mechanisms of the discrete model. As suggested by literature, the irregularities in the vegetation patterns may result from the spatiotemporal chaos, which is an important natural phenomenon widely observed [25, 34, 35].

Figure 6 also shows the change of striped vegetation patterns with parameters a and d. With reduction of a or d, the striped patterns experience a transition from regular stripes, to curved stripes, and to fractured stripes. More precipitation (a rising) leads to the increase in stripe numbers, which suggests a great enhancement of biomass in the patterns. To quantitatively determine the influence of parameter variations, two important characteristics of the striped vegetation patterns on hillslopes, wavelength and migrating speed, are studied. When the values/ranges of parameters a, m, and v are taken from Table 2, the ranges of wavelength and migrating speed for the irregular striped vegetation patterns are the same with that in Table 3. Therefore, our results are comparable with the natural striped patterns in semiarid regions.

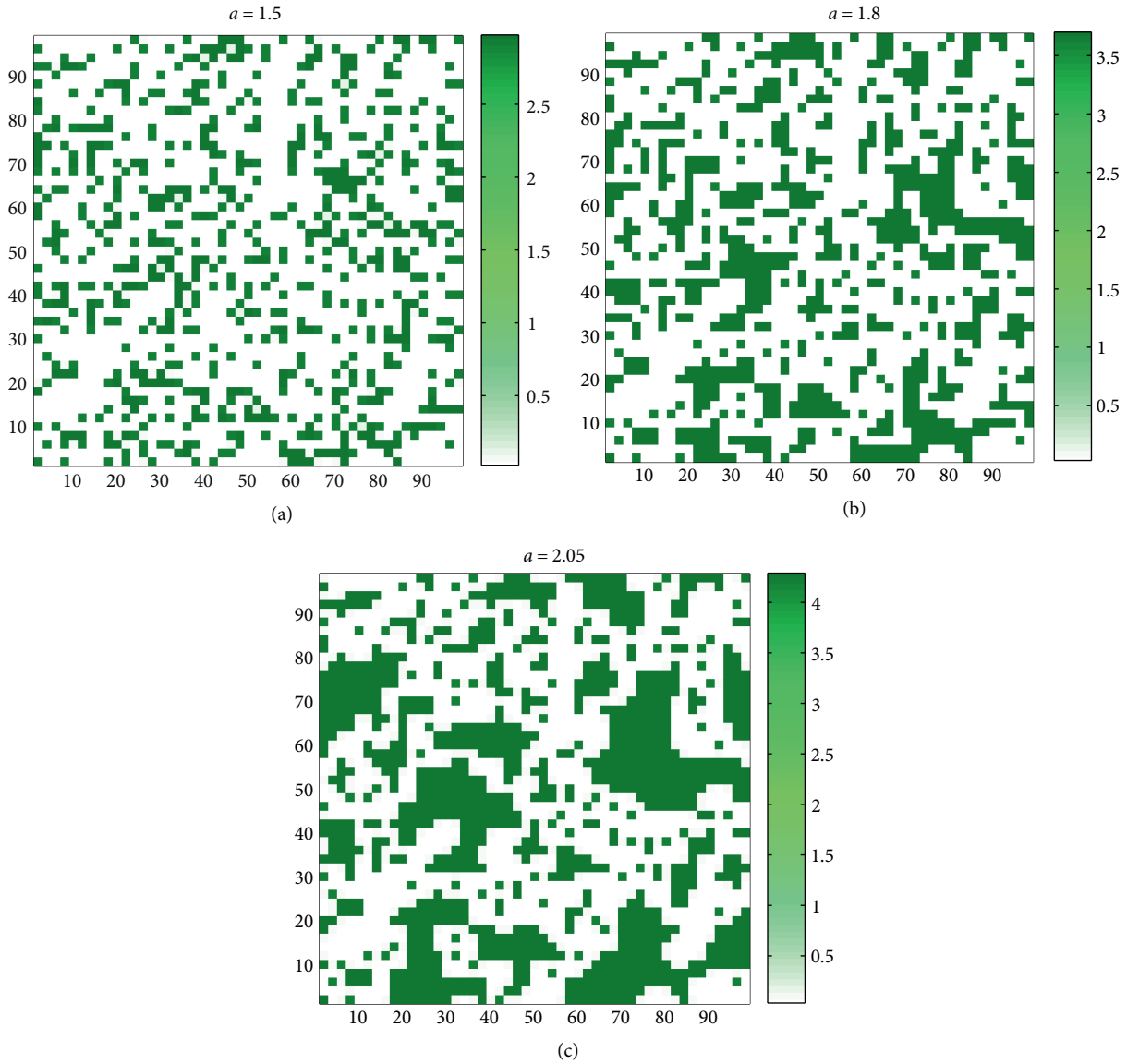

FIGURE 5: Patterns of irregular patches on flat ground, with application of same initial condition (IC2). $m = 0.45$, $d = 0.003$, $t = 1000$.

Figures 6(g) and (h) show the irregular spotted vegetation patterns self-organized on hillslopes. In the patterns, the distribution of vegetation spots shows irregular characteristic. Compared with the striped patterns, the values of d for formation of spotted patterns are much smaller. In such cases, low diffusion capability restrains the lateral vegetation dispersal and the development of vegetation stripes. In literature, spotted shrubby patterns on hillslopes are observed in Central Morocco by D'Odorico et al. [45] and in Israel by Shnerb et al. [51]. Compared with field observations and considering the parametric conditions applied in this research, Figures 6(g) and (h) tend to describe the spotted patterns of perennial shrubs. Moreover, Figures 6(g) and (h) show denser vegetation spots as rainfall increases. This also agrees with the field observation recorded by Shnerb et al. [51]. However, few theoretical models are capable of reproducing the formation of spotted vegetation patterns on hillslopes [45, 51].

The spotted vegetation patterns keep stationary as time progresses. This is opposite to the migrating property of striped patterns. Such contrast is induced by different diffusion capabilities of vegetation. Stronger diffusion can lead to successful colonization of plants in bare areas. As observed in filed investigation [12], the migration of striped patterns takes place when colonization of bare areas occurs at the moister upslope side of vegetation stripes, whereas the plants on the downslope side of stripes die due to inadequate water [13]. However, while diffusion capability is weak, the lateral vegetation dispersal is restrained. When the colonization-dying process cannot happen, stationary patterns will emerge, as demonstrated by the stationary spotted patterns. As indicated by literature, the nonlinear mechanism for self-organization of the stationary patterns is spatiotemporal chaos [34]. Moreover, a frozen random chaos can be identified in Figures 6(g) and (h) according to the classification of the spatiotemporal chaos [52].

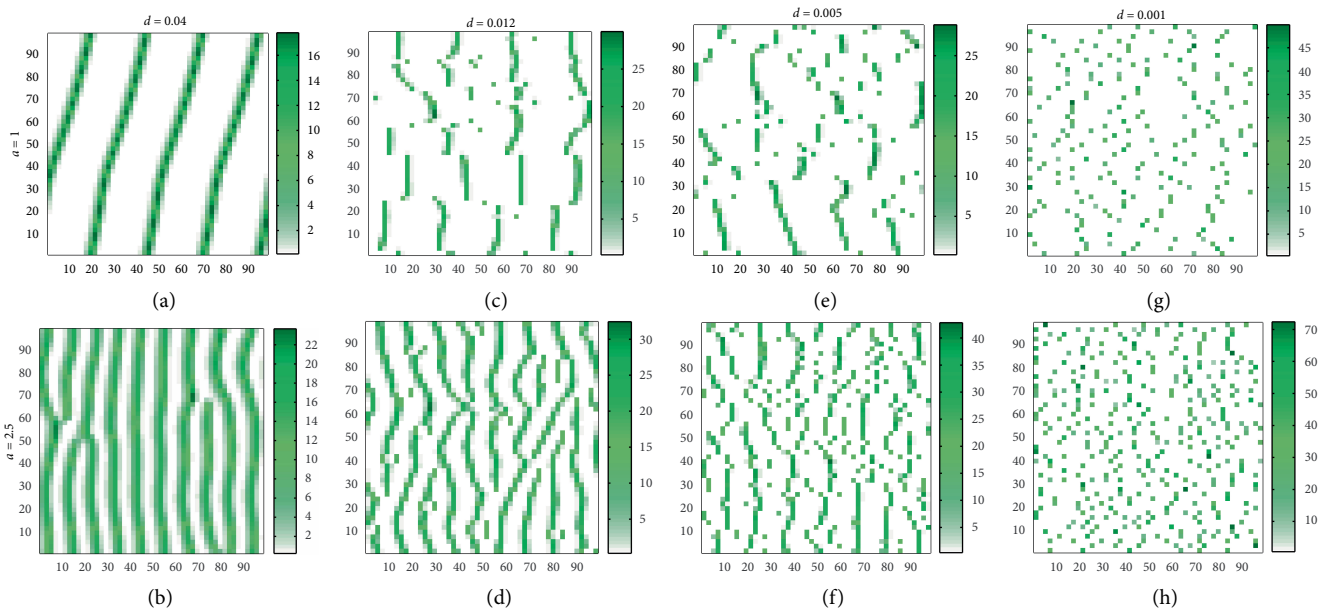

FIGURE 6: Irregular vegetation patterns self-organized on hillslopes as values of a and d shift, under the same initial condition (IC1). Application of IC2 can obtain similar results as well. $m = 0.45$, $v = 45.625$, $t = 1000$.

The migrating and stationary patterns on hillslopes described by the discrete model agree with the prediction by many models [13, 43]. However, the evidence of upslope migration in vegetation patterns remains scare in direct field observations [3, 4, 44]. A few researchers also investigate the formation of stationary vegetation patterns on hillslopes [16, 44]. The stationary patterns predicted in literature may need introduction of complex mechanisms, such as secondary seed dispersal [16]. With application of simple feedback mechanisms of water and biomass, the discrete model has power to predict both migrating and stationary vegetation patterns on hillslopes, merely via parameter variations.

Inferred from the transition from striped patterns to spotted patterns, an intermediate pattern, striped-spotted vegetation pattern, is suggested. Such type of patterns shows coexistence of vegetation spots and stripes, as shown in Figures 6(e) and (f). The occurrence of such patterns confirms the transition between spotted and striped patterns, as rainfall rate or vegetation diffusion capability changes. This mechanism suggests that rainfall and vegetation types play an important role in the formation of vegetation patterns.

The parameter variations exert a key influence on the transition of vegetation patterns on hillslopes. Two aspects of pattern transition with parameter variations can be found in Figure 6. First, increase in rainfall enhances vegetation biomass in patterns, as widely observed in nature [49, 51]. The enhancement of biomass affects the characteristics of vegetation patterns. For striped vegetation patterns, the wavelength reduces and number of vegetation stripes increases [49]; whereas for spotted vegetation patterns, denser spotted vegetation patches can be observed and aggregation of vegetation takes place [51]. Second, decrease in vegetation diffusion capability promotes fragmentation of vegetation patterns, causing the transition from striped pattern to spotted pattern. However, such phenomenon is seldom described in literature, but exhibited by the present discrete model. Via the influence of parameter variations on vegetation patterns, the discrete model captures the formation of diverse vegetation patterns in semiarid regions, under different rainfall conditions and for various vegetation types.

Notice that the above results are related to the grass pattern formation in semiarid regions. When we perform numerical simulations with the parameter values representing trees ($a_{\text{tree}} = 0.091 - 0.23$ and $m_{\text{tree}} = 0.045$), similar results can be obtained both on the flat ground and on the hillslopes.

5. Conclusion

A space- and time-discrete model is developed in this research for studying the vegetation pattern formation in semiarid regions. Turing-type instability analysis produces the pattern formation conditions. Numerical simulations performed based on the model reveal self-organization of many vegetation patterns, such as regular mosaic, irregular patched, striped, spotted, fractured striped and striped-spotted on flat ground or on hillslopes. Based on the findings in this research, the following should be addressed.

(1) The discrete model shows great advantage in describing vegetation pattern formation. Relying on nonlinear mechanism of the discrete model, vegetation patterns of mosaic, irregular patches, curved and fractured stripes, and spots are found.

(2) Parameter variations result to transition of vegetation patterns. Variations of rainfall rate and vegetation diffusion capability affect two different characteristics of vegetation patterns, causing occurrence of diverse vegetation patterns.

(i) Increase in rainfall enhances biomass in vegetation patterns. Simultaneously, the characteristics of patterns are influenced. For irregular patched patterns, the vegetation patches enlarge; for striped patterns, wavelengths reduce; and for spotted patterns, vegetation spots become denser.

(ii) Decrease in vegetation diffusion capability affects vegetation patterns in two aspects. First, it promotes the fragmentation of patterns, causing the transition from striped patterns to striped-spotted patterns, and to spotted patterns. Second, it can lead to the transition from migrating patterns to stationary patterns. Such result is seldom described in literature and new predicted by the discrete Klausmeier model.

Via comparison, the simulated results obtained in this research agree with many records of field observations as described in literature. The agreement mainly reflects in the following two aspects.

(1) *Pattern configurations:* on flat ground, the simulated mosaic pattern is similar to the natural gap vegetation pattern as described in Rietkerk et al. [43] and Kéfi et al. [46], whereas the simulated patched vegetation patterns likely mimic that observed by Cerdà [47]. On hillslopes, we obtain regular, curved and fractured striped vegetation patterns, which are widely recorded in direct field observations of semiarid grass and trees [4, 13]. As well, the spotted patterns are simulated on hillslopes, and such type of pattern is close to the spotted shrubby patterns as observed by D'Odorico et al. [45] and Shnerb et al. [51].

(2) *Pattern characteristics:* with feasible parameter values/ranges (see Tables 1 and 2), the ranges of wavelength and migrating speed for the striped patterns are close to the observations of the natural striped vegetation patterns in semiarid regions (see Table 3). Moreover, spotted patterns on hillslopes are simulated to be stationary. Since the evidence of upslope migration in vegetation patterns remains scare in direct field observations [3, 4, 44], the stationary vegetation patterns on hillslopes may be common and the discrete model provides a new nonlinear mechanism for explaining the self-organization of hillslope stationary patterns.

As well known, the competing interactions at different spatial scales can be the main mechanism which promotes the self-organization of stable patterns [53–56]. In this research, the discrete model also includes such competing interactions. On the one hand, the short-range dispersal of vegetation drives the expansion of vegetation patches; on the other hand, the long-range flow of water leads to spatial redistribution of water resource, which constrains the expansion of vegetation patches due to the competition for water among different patches. Under the influence of both short-range dispersal of vegetation and long-range flow of water, a patch of vegetation can erupt as well as be restrained in expansion. When the spatial equilibrium reaches, vegetation patterns are self-organized and can maintain stable.

The self-organized vegetation patterns and the transitions of patterns result from essential nonlinear mechanisms of the discrete model. With the improvements upon former theoretical models, the discrete model developed and its nonlinear mechanisms contribute advantages in analyzing and describing the complexity of vegetation pattern formation in semiarid regions.

Appendix

A. Local Stability of Fixed Points

With consideration of $\nabla_D w_t^{ij} \equiv 0$ and $\nabla^D{}_2 u_t^{ij} \equiv 0$, Eq. (8a) and (8b) transforms into the following,

$$\begin{aligned} 0 &= a - w_t^{ij} - w_t^{ij}\left(u_t^{ij}\right)^2, \\ u_{t+1}^{ij} &= (1-m)u_t^{ij} + w_t^{ij}\left(u_t^{ij}\right)^2. \end{aligned} \tag{A.1}$$

Mathematically, the homogeneous stationary states of the discrete model are represented by the fixed points of Eq. (A.1). According to the definition of fixed point [57], the fixed points of Eq. (A.1) are solved by

$$\begin{aligned} 0 &= a - w - wu^2, \\ u &= (1-m)u + wu^2, \end{aligned} \tag{A.2}$$

Calculation on Eq. (A.2) obtains three fixed points when $a > 2m$ (see Eq. (9)). Then the stability of the spatially homogeneous stationary states with respect to spatially homogeneous perturbations is analyzed. For spatially homogeneous perturbations, $\nabla_D w_t^{ij} \equiv 0$ and $\nabla^D{}_2 u_t^{ij} \equiv 0$ still establish. From Eq. (A.1), the following dynamic equation is obtained,

$$u_{t+1}^{ij} = (1-m)u_t^{ij} + \frac{a\left(u_t^{ij}\right)^2}{1+\left(u_t^{ij}\right)^2}. \tag{A.3}$$

The Jacobian determinant of Eq. (A.3) is described by

$$J = (1-m) + \frac{2au}{\left(1+u^2\right)^2}. \tag{A.4}$$

Stable fixed point of Eq. (A.1) should satisfy the following conditions,

$$\left|J(u^*)\right| = \left|(1-m) + \frac{2au^*}{\left(1+u^{*2}\right)^2}\right| < 1, \tag{A.5}$$

in which u^* takes the biomass value of either u_1 or u_2. Straight calculation on Eq. (A.5) suggests that the fixed point (w_1, u_1) cannot be stable whereas the fixed point (w_2, u_2) can be stable. The conditions for stable fixed point (w_2, u_2) are described in Eq. (10a and 22b).

B. Linearization of Eq. (8)

Firstly based on previous research works [58–60], the eigenvalues of operators ∇_D and $\nabla^D{}_2$ can be provided as

$$\begin{aligned} \lambda_{kl}^{(1)} &= 2\sin\phi_k \exp\left(\left(\phi_k - \tfrac{\pi}{2}\right)i'\right), \\ \lambda_{kl}^{(2)} &= 4\left(\sin^2\phi_k + \sin^2\phi_l\right), \end{aligned} \tag{B.1}$$

in which $\phi_k = (k-1)\pi/n\, i' = \sqrt{-1}$, and $k, l \in \{1, 2, 3, \cdots, n\}$. Moreover, it can be verified that

$$\nabla_D\left(\nabla^D{}_2\left(X^{ij}\right)\right) = \nabla_D^2\left(\nabla_D\left(X^{ij}\right)\right). \tag{B.2}$$

This implies that ∇_D^2 and ∇_D are commuting operators. Therefore, the two operators have a common set of eigenfunctions. Let X_{kl}^{ij} be the common eigenfunction of the eigenvalues $\lambda_{kl}^{(1)}$ and $\lambda_{kl}^{(2)}$.

Then considering spatially heterogeneous perturbations around the spatially homogeneous state $(w_2,\ u_2)$, i.e.,

$$\begin{aligned} w_t^{ij} &= w_2 + \tilde{w}_t^{ij}, \\ u_t^{ij} &= u_2 + \tilde{u}_t^{ij}, \end{aligned} \tag{B.3}$$

in which $\tilde{w}_t^{ij}$ and $\tilde{u}_t^{ij}$ are the perturbations of water and biomass in cell (i, j) at time t. Substituting Eq. (B.3) into Eq. (8a) and (8b), and noticing that

$$\begin{aligned} \nabla_D w_t^{ij} &= \nabla_D \tilde{w}_t^{ij}, \\ \nabla^D{}_2 u_t^{ij} &= \nabla^D{}_2 \tilde{u}_t^{ij}, \end{aligned} \tag{B.4}$$

the following can be obtained,

$$\begin{aligned} 0 &= a_{11}\tilde{w}_t^{ij} + a_{12}\left(\tilde{u}_t^{ij} + d\nabla^D{}_2\tilde{u}_t^{ij}\right) + \nu\nabla_D\tilde{w}_t^{ij} + o\left(\tilde{w}_t^{ij} + \tilde{u}_t^{ij}\right), \\ \tilde{u}_{t+1}^{ij} &= a_{21}\tilde{w}_t^{ij} + a_{22}\left(\tilde{u}_t^{ij} + d\nabla_D^2\tilde{u}_t^{ij}\right) + o\left(\tilde{w}_t^{ij} + \tilde{u}_t^{ij}\right), \end{aligned} \tag{B.5}$$

in which

$$\begin{aligned} a_{11} &= -1 - u_2^2, \\ a_{12} &= -2w_2u_2, \\ a_{21} &= u_2^2, \\ a_{22} &= 1 - m + 2w_2u_2, \end{aligned} \tag{B.6}$$

$o\left(\tilde{w}_t^{ij} + \tilde{u}_t^{ij}\right)$ represents high order terms of $\tilde{w}_t^{ij}$ and $\tilde{u}_t^{ij}$. When the perturbations are weak, $o\left(\tilde{w}_t^{ij} + \tilde{u}_t^{ij}\right)$ can be ignored in the following calculations. Using X_{kl}^{ij} to multiply Eq. (B.5) gets

$$\begin{aligned} 0 &= a_{11}X_{kl}^{ij}\tilde{w}_t^{ij} + a_{12}X_{kl}^{ij}\tilde{u}_t^{ij} + da_{12}X_{kl}^{ij}\nabla^2\tilde{u}_t^{ij} + \nu X_{kl}^{ij}\nabla\tilde{w}_t^{ij}, \\ X_{kl}^{ij}\tilde{u}_{t+1}^{ij} &= a_{21}X_{kl}^{ij}\tilde{w}_t^{ij} + a_{22}X_{kl}^{ij}\tilde{u}_t^{ij} + da_{22}X_{kl}^{ij}\nabla^2\tilde{u}_t^{ij}. \end{aligned} \tag{B.7}$$

Summing Eq. (B.7) for all of i and j obtains

$$\begin{aligned} 0 &= a_{11}\sum_{i,j=1}^{n} X_{kl}^{ij}\tilde{w}_t^{ij} + a_{12}\sum_{i,j=1}^{n} X_{kl}^{ij}\tilde{u}_t^{ij} \\ &\quad + da_{12}\sum_{i,j=1}^{n} X_{kl}^{ij}\nabla^2\tilde{u}_t^{ij} + \nu\sum_{i,j=1}^{n} X_{kl}^{ij}\nabla\tilde{w}_t^{ij}, \\ \sum_{i,j=1}^{n} X_{kl}^{ij}\tilde{u}_{t+1}^{ij} &= a_{21}\sum_{i,j=1}^{n} X_{kl}^{ij}\tilde{w}_t^{ij} + a_{22}\sum_{i,j=1}^{n} X_{kl}^{ij}\tilde{u}_t^{ij} + da_{22}\sum_{i,j=1}^{n} X_{kl}^{ij}\nabla^2\tilde{u}_t^{ij}. \end{aligned} \tag{B.8}$$

Let $W_t = \sum_{i,j=1}^{n} X_{kl}^{ij}\tilde{w}_t^{ij}$ and $U_t = \sum_{i,j=1}^{n} X_{kl}^{ij}\tilde{u}_t^{ij}$, Eq. (B.8) can be transformed into the following form under the consideration of the periodic boundary conditions shown in Eq. (8c) and (8d) [27],

$$\begin{aligned} 0 &= \left(a_{11} - \nu\lambda_{kl}^{(1)}\right)W_t + a_{12}\left(1 - d\lambda_{kl}^{(2)}\right)U_t, \\ U_{t+1} &= a_{21}W_t + a_{22}\left(1 - d\lambda_{kl}^{(2)}\right)U_t. \end{aligned} \tag{B.9}$$

Data Availability

The data of system parameter values and striped vegetation pattern characteristics have been previously reported and are available at DOI: https://doi.org/10.1126/science.284.5421.1826. These data are used to support the numerical simulations of this study, and the prior study is cited at relevant places within the text as reference. In addition, with the system parameter values determined by the data, numerical simulations are performed and the results of vegetation pattern formation are generated during the simulation study.

Conflicts of Interest

The authors declare that they have no conflicts of interest.

Funding

This research was financed by the National Water Pollution Control and Treatment Science and Technology Major Project (No. 2017ZX07101-002), the National Natural Science Foundation of China (No. 11802093), and the Fundamental Research Funds for the Central Universities (No. JB2017069).

References

[1] J. A. Mabbut and P. C. Fanning, "Vegetation banding in arid western Australia," *Journal of Arid Environments*, vol. 12, pp. 41–59, 1987.

[2] A. Mauchamp and J. L. Janeau, "Water funneling by the crown of Flourensia cernua, a Chihuahuan Desert shrub," *Journal of Arid Environments*, vol. 25, pp. 299–306, 1993.

[3] D. L. Dunkerley and K. J. Brown, "Runoff and runon areas in a patterned chenopod shrubland, arid western New South Wales, Australia: characteristics and origin," *Journal of Arid Environments*, vol. 30, no. 1, pp. 41–55, 1995.

[4] C. Valentin, J. M. d'Herbès, and J. Poesen, "Soil and water components of banded vegetation patterns," *Catena*, vol. 37, no. 1–2, pp. 1–24, 1999.

[5] R. HilleRisLambers, M. Rietkerk, F. van den Bosch, H. Prins, and H. de Kroon, "Vegetation pattern formation in semi-arid grazing systems," *Ecology*, vol. 82, pp. 50–61, 2001.

[6] J. A. Ludwig and D. J. Tongway, "Spatial organisation of landscapes and its function in semi-arid woodlands, Australia," *Landscape Ecology*, vol. 10, no. 1, pp. 51–63, 1995.

[7] J. A. Ludwig, D. J. Tongway, and S. G. Mardsen, "Stripes, strands or stipples: modelling the influence of three landscape banding patterns on resource capture and productivity in semi-arid woodlands, Australia," *Catena*, vol. 37, no. 1–2, pp. 257–273, 1999.

[8] J. A. Ludwig, B. P. Wilcox, D. D. Breshears, D. J. Tongway, and A. C. Imeson, "Vegetation patches and runoff-erosion as interacting ecohydrological processes in semiarid landscapes," *Ecology*, vol. 86, no. 2, pp. 288–297, 2005.

[9] F. Borgogno, P. D'Odorico, F. Laio, and L. Ridolfi, "Mathematical models of vegetation pattern formation in ecohydrology," *Reviews of Geophysics*, vol. 47, no. 1, Article ID RG1005, 2009.

[10] K. Siteur, E. Siero, M. B. Eppinga, J. D. M. Rademacher, A. Doelman, and M. Rietkerk, "Beyond Turing: the response of patterned ecosystem to environmental change," *Ecological Complexity*, vol. 20, pp. 81–96, 2014.

[11] D. Caracciolo, L. V. Noto, E. Istanbulluoglu, S. Fatichi, and X. Zhou, "Climate change and Ecotone boundaries: insights from a cellular automata ecohydrology model in a Mediterranean catchment with topography controlled vegetation patterns," *Advances in Water Resources*, vol. 73, pp. 159–175, 2014.

[12] J. Thiéry, J.-M. d'Herbès, and C. Valentin, "A model for simulating the genesis of banded patterns in Niger," *Journal of Ecology*, vol. 83, no. 3, pp. 497–507, 1995.

[13] C. A. Klausmeier, "Regular and irregular patterns in semiarid vegetation," *Science*, vol. 284, no. 5421, pp. 1826–1828, 1999.

[14] E. Gilad, J. von Hardenberg, A. Provenzale, M. Shachak, and E. Meron, "Ecosystem engineers: from pattern formation to habitat creation," *Physical Review Letters*, vol. 93, no. 9, Article ID 098105, 2004.

[15] E. Meron, E. Gilad, J. von Hardenberg, M. Shachak, and Y. Zarmi, "Vegetation patterns along a rainfall gradient," *Chaos, Solitons & Fractals*, vol. 19, no. 2, pp. 367–376, 2004.

[16] S. Thompson and G. Katul, "Secondary seed dispersal and its role in landscape organization," *Geophysical Research Letters*, vol. 36, no. 2, Article ID L02402, 2009.

[17] S. Kéfi, M. B. Eppinga, P. C. de Ruiter, and M. Rietkerk, "Bistability and regular spatial patterns in arid ecosystems," *Theoretical Ecology*, vol. 3, no. 4, pp. 257–269, 2010.

[18] J. von Hardenberg, A. Y. Kletter, H. Yizhaq, J. Nathan, and E. Meron, "Periodic versus scale-free patterns in dryland vegetation," *Proceedings of the Royal Society B: Biological Sciences*, vol. 277, no. 1688, pp. 1771–1776, 2010.

[19] J. A. Sherratt, "An analysis of vegetation stripe formation in semi-arid landscapes," *Journal of Mathematical Biology*, vol. 51, no. 2, pp. 183–197, 2005.

[20] J. A. Sherratt, "Pattern solutions of the Klausmeier Model for banded vegetation in semi-arid environments I," *Nonlinearity*, vol. 23, no. 10, pp. 2657–2675, 2010.

[21] J. A. Sherratt, "Pattern solutions of the Klausmeier Model for banded vegetation in semi-arid environments II: patterns with the largest possible propagation speeds," *Proceedings of the Royal Society A: Mathematical, Physical and Engineering Sciences*, vol. 467, no. 2135, pp. 3272–3294, 2011.

[22] J. A. Sherratt, "Pattern solutions of the Klausmeier Model for banded vegetation in semi-arid environments III: the transition between homoclinic solutions," *Physica D: Nonlinear Phenomena*, vol. 242, no. 1, pp. 30–41, 2013.

[23] S. Kondo and T. Miura, "Reaction-diffusion model as a framework for understanding biological pattern formation," *Science*, vol. 329, no. 5999, pp. 1616–1620, 2010.

[24] P. Comer, D. Faber-Langendoen, R. Evans et al., *Ecological Systems of the United States: A Working Classification of U.S. Terrestrial Systems*, NatureServe, Arlington, VA, 2003.

[25] D. C. Mistro, L. A. D. Rodrigues, and S. Petrovskii, "Spatiotemporal complexity of biological invasion in a space- and time-discrete predator-prey system with the strong Allee effect," *Ecological Complexity*, vol. 9, pp. 16–32, 2012.

[26] G. Domokos and I. Scheuring, "Discrete and continuous state population models in a noisy world," *Journal of Theoretical Biology*, vol. 227, no. 4, pp. 535–545, 2004.

[27] Y.-T. Han, B. Han, L. Zhang, L. Xu, M.-F. Li, and G. Zhang, "Turing instability and wave patterns for a symmetric discrete competitive Lotka-Volterra system," *WSEAS Transactions on Mathematics*, vol. 10, pp. 181–189, 2011.

[28] M. Li, B. Han, L. Xu, and G. Zhang, "Spiral patterns near Turing instability in a discrete reaction diffusion system," *Chaos, Solitons & Fractals*, vol. 49, pp. 1–6, 2013.

[29] R. M. May, "Simple mathematical models with very complicated dynamics," *Nature*, vol. 261, pp. 459–467, 1976.

[30] W. Gibson and W. G. Wilson, "Individual-based chaos: existence of the discrete logistic model," *Journal of Theoretical Biology*, vol. 339, pp. 84–92, 2013.

[31] R. Mancy, P. Prosser, and S. Rogers, "Discrete and continuous time simulations of spatial ecological processes predict different final population sizes and interspecific competition outcomes," *Ecological Modelling*, vol. 259, pp. 50–61, 2013.

[32] P. P. Saratchandran, K. C. Ajithprasad, and K. P. Harikrishnan, "Numerical exploration of the parameter plane in a discrete predator-prey model," *Ecological Complexity*, vol. 21, pp. 112–119, 2015.

[33] J. Puigdefabregas, F. Gallart, O. Biaciotto, M. Allogia, and G. del Barrio, "Banded vegetation patterning in a subantarctic forest of Tierra del Fuego, as an outcome of the interaction between wind and tree growth," *Acta Oecologica*, vol. 20, no. 3, pp. 135–146, 1999.

[34] D. Punithan, D. K. Kim, and R. I. B. McKay, "Spatio-temporal dynamics and quantification of daisyworld in two-dimensional coupled map lattices," *Ecological Complexity*, vol. 12, pp. 43–57, 2012.

[35] L. A. D. Rodrigues, D. C. Mistro, and S. Petrovskii, "Pattern formation in a space- and time-discrete predator-prey system with a strong Allee effect," *Theoretical Ecology*, vol. 5, no. 3, pp. 341–362, 2012.

[36] Z. He and X. Lai, "Bifurcation and chaotic behavior of a discrete-time predator-prey system," *Nonlinear Analysis: Real World Applications*, vol. 12, no. 1, pp. 403–417, 2011.

[37] L. Zhang, C. Zhang, and M. Zhao, "Dynamic complexities in a discrete predator-prey system with lower critical point for the prey," *Mathematics and Computers in Simulation*, vol. 105, pp. 119–131, 2014.

[38] A. M. Turing, "The chemical basis of morphogenesis," *Philosophical Transactions of the Royal Society of London, Series B*, vol. 237, pp. 37–72, 1952.

[39] Q. Bie, Q. Wang, and Z. Yao, "Cross-diffusion induced instability and pattern formation for a Holling type-II predator-prey model," *Applied Mathematics and Computation*, vol. 247, pp. 1–12, 2014.

[40] T. Huang, H. Zhang, H. Yang, N. Wang, and F. Zhang, "Complex patterns in a space- and time-discrete predator-prey model with Beddington-DeAngelis functional response," *Communications in Nonlinear Science and Numerical Simulation*, vol. 43, pp. 182–199, 2017.

[41] T. Huang, H. Zhang, and H. Yang, "Spatiotemporal complexity of a discrete space-time predator-prey system with self- and cross-diffusion," *Applied Mathematical Modelling*, vol. 47, pp. 637–655, 2017.

[42] T. Huang, H. Yang, H. Zhang, X. Cong, and G. Pan, "Diverse self-organized patterns and complex pattern transitions in a discrete ratio-dependent predator-prey system," *Applied Mathematics and Computation*, vol. 326, pp. 141–158, 2018.

[43] M. Rietkerk, M. C. Boerlijst, F. van Langevelde et al., "Self-organization of vegetation in arid ecosystems," *The American Naturalist*, vol. 160, no. 4, pp. 524–530, 2002.

[44] P. M. Saco, G. R. Willgoose, and G. R. Hancock, "Eco-geomorphology of banded vegetation patterns in arid and semi-arid regions," *Hydrology and Earth System Sciences*, vol. 11, no. 6, pp. 1717–1730, 2007.

[45] P. D'Odorico, F. Laio, and L. Ridolfi, "Patterns as indicators of productivity enhancement by facilitation and competition in dryland vegetation," *Journal of Geophysical Research*, vol. 111, Article ID G03010, 2006.

[46] S. Kéfi, M. Rietkerk, C. L. Alados et al., "Spatial vegetation patterns and imminent desertification in Mediterranean arid ecosystems," *Nature*, vol. 449, no. 7159, pp. 213–217, 2007.

[47] A. Cerdà, "The effect of patchy distribution of *Stipatenacissima* L. on runoff and erosion," *Journal of Arid Environments*, vol. 36, no. 1, pp. 37–51, 1997.

[48] P. D'Odorico, F. Laio, and L. Ridolfi, "Vegetation patterns induced by random climate fluctuations," *Geophysical Research Letters*, vol. 33, no. 19, Article ID L19404, 2006.

[49] J. von Hardenberg, E. Meron, M. Shachak, and Y. Zarmi, "Diversity of vegetation patterns and desertification," *Physical Review Letters*, vol. 87, no. 19, Article ID 198101, 2001.

[50] N. Barbier, P. Couteron, R. Lefever, V. Deblauwe, and O. Lejeune, "Spatial decoupling of facilitation of facilitation and competition at the origin of gapped vegetation patterns," *Ecology*, vol. 89, pp. 1521–1531, 2008.

[51] N. M. Shnerb, P. Sarah, H. Lavee, and S. Solomon, "Reactive glass and vegetation patterns," *Physical Review Letters*, vol. 90, no. 3, Article ID 038101, 2003.

[52] L. Xu, G. Zhang, B. Han, L. Zhang, M. F. Li, and Y. T. Han, "Turing instability for a two-dimensional logistic coupled map lattice," *Physics Letters A*, vol. 374, no. 34, pp. 3447–3450, 2010.

[53] W. G. Wilson, A. M. Deroos, and E. McCauley, "Spatial instabilities within the diffusive Lotka–Volterra system: individual-based simulation results," *Theoretical Population Biology*, vol. 43, no. 1, pp. 91–127, 1993.

[54] W. G. Wilson, "Resolving discrepancies between deterministic population models and individual-based simulations," *The American Naturalist*, vol. 151, no. 2, pp. 116–134, 1998.

[55] W. G. Wilson, S. P. Harrison, A. Hastings, and K. McCann, "Stable pattern formation in tussock moth populations," *Journal of Animal Ecology*, vol. 68, pp. 94–107, 1999.

[56] W. G. Wilson, W. F. Morris, and J. L. Bronstein, "Coexistence of mutualists and exploiters on spatial landscapes," *Ecological Monographs*, vol. 73, no. 3, pp. 397–413, 2003.

[57] A. H. Nayfeh and B. Balachandran, *Applied Nonlinear Dynamics: Analytical, Computational, and Experimental Methods*, Wiley Interscience, 1995.

[58] L. Bai and G. Zhang, "Nontrivial solutions for a nonlinear discrete elliptic equation with periodic boundary conditions," *Applied Mathematics and Computation*, vol. 210, no. 2, pp. 321–333, 2009.

[59] T. Huang, X. Cong, H. Zhang, S. Ma, and G. Pan, "Pattern self-organization and pattern transition on the route to chaos in a spatiotemporal discrete predator-prey system," *Advances in Difference Equations*, vol. 2018, no. 1, Article ID 175, 2018.

[60] T. Huang, H. Zhang, X. Cong, G. Pan, X. Zhang, and Z. Liu, "Exploring spatiotemporal complexity of a predator-prey system with migration and diffusion by a three-chain coupled map lattice," *Complexity*, vol. 2019, Article ID 3148323, 19 pages, 2019.

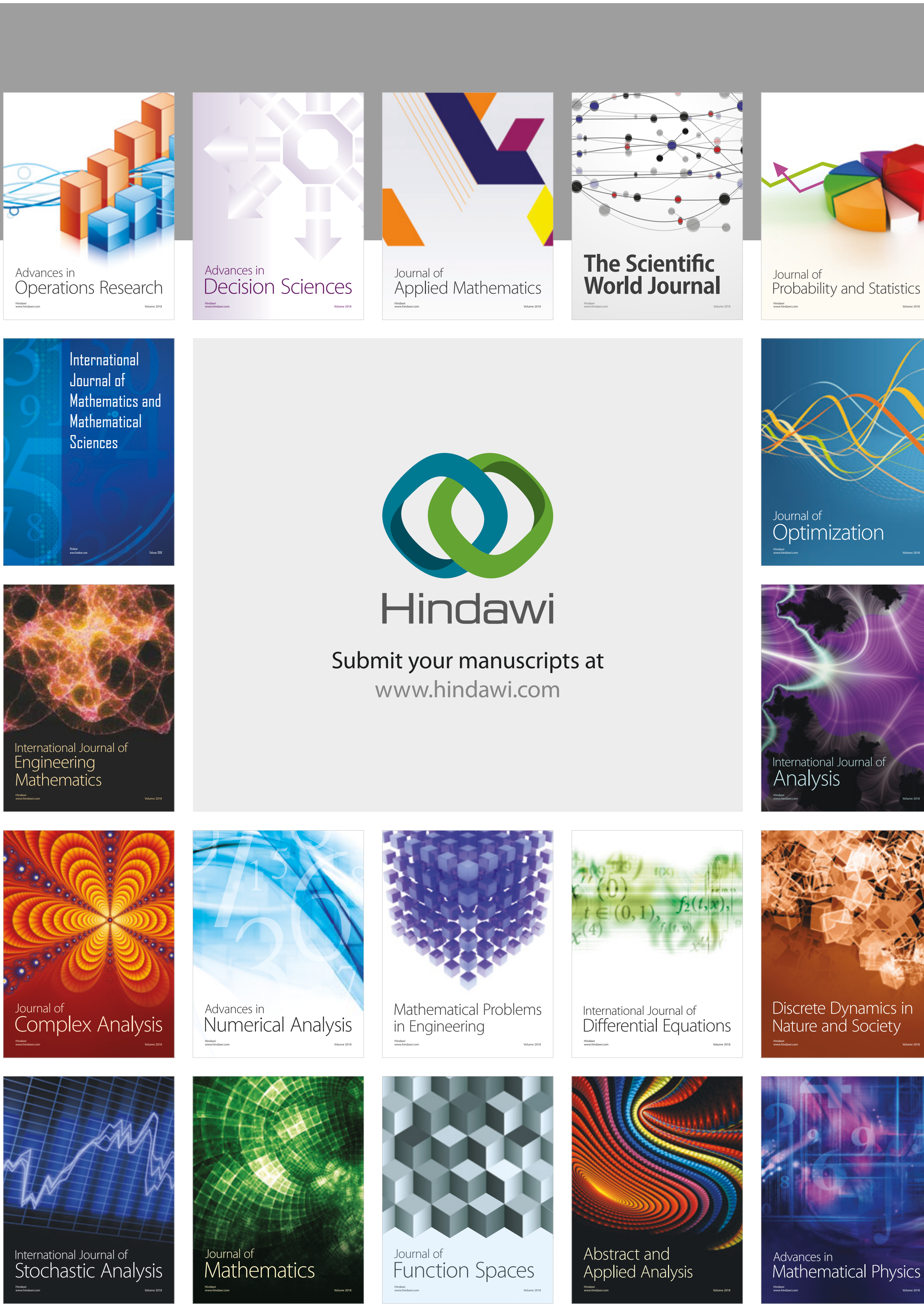
Advances in
Operations Research
Advances in
Decision Sciences
Journal of
Applied Mathematics
The Scientific
World Journal
Journal of
Probability and Statistics
International
Journal of
Mathematics and
Mathematical
Sciences
Hindawi
Submit your manuscripts at
www.hindawi.com
Journal of
Optimization
International Journal of
Engineering
Mathematics
International Journal of
Analysis
Journal of
Complex Analysis
Advances in
Numerical Analysis
Mathematical Problems
in Engineering
International Journal of
Differential Equations
Discrete Dynamics in
Nature and Society
International Journal of
Stochastic Analysis
Journal of
Mathematics
Journal of
Function Spaces
Abstract and
Applied Analysis
Advances in
Mathematical Physics